



www.ericjournal.ait.ac.th

Energy-Saving Analysis of a Hybrid-Power Gas Engine Heat Pump with Continuously Variable Transmission

Tao Chen^{*1} and Liang Cai^{*}

Abstract – Hybrid-power gas engine heat pump (HPGHP) could achieve the efficient operation of the engine and improve the partial load performance of the air conditioning system through the cooperation of the gas engine and the dual-use motor. In the paper, the continuously variable transmission is applied to a coaxial parallel HPGHP system to analyze the influence of transmission mechanism on the operating characteristics, and an instantaneous optimal control strategy aiming at minimizing the equivalent energy consumption is proposed to complete the torque distribution of the engine and the motor. The results show that the compressor speed of 1350 rpm and 1800 rpm are the switching point of three operating modes under the specified heating conditions, and the engine torque and gas consumption rate maintained at relatively stable values of 29.5 N·m and 284 g·(kW·h) by means of the motor with high efficiency in the wide torque range, showing the good energy saving effect.

Keywords – control strategy, CVT, equivalent energy consumption minimization, HPGHP, instantaneous optimization.

1. INTRODUCTION

Nowadays, the problems of energy consumption and environmental pollution caused by heating and cooling in residential and industrial facilities have attracted more and more people's attention [1]. Gas engine-driven heat pump (GEHP) system is a kind of vapor compression heat pump driven by gas engine, due to its high partial load performance and primary energy ratio (PER), is widely utilized in the process of cooling, heating or food drying [2]-[4]. However, when the building load fluctuates too large or too small, the operating conditions of gas engine will deviate from its economic zone, resulting in poor stability, lower thermal efficiency and heavier emissions [5]. Therefore, hybrid-power gas engine-driven heat pump (HPGHP) system is first proposed by the Air Conditioning and Refrigeration Laboratory of Southeast University, which can achieve the stable operation of the gas engine through the cooperation of the auxiliary power battery [6].

Performance studies show that HPGHP has a relatively low fuel consumption rate and higher thermal efficiency than conventional gas heat pumps [7]. The role of energy management strategy is to achieve switching of work modes and distribution of torque according to the performance characteristics of the power components and the operation status of the heat pump system [8], which determines the fuel economy and energy-saving potential of the HPGHPs [9]. An instantaneous optimal control strategy based on equivalent gas conversion efficiency of drive system was proposed to determine the switching point between the modes according to the intersection of the equivalent gas consumption rate under different modes [10]. An engine optimal torque control strategy for achieving

minimum fuel consumption was presented, arguing that the system is the most economical when the engine is running on the optimal torque curve [11]. Further comparisons found that the energy-saving effect of HPGHPs under the engine optimal torque control strategy is about 4% higher than that of the engine economic zone control strategy under the same load [12].

The above literature on the operating characteristics and energy-saving analysis of HPGHP system are all about multi-stage gear transmission, which cannot achieve real-time matching of engine speed and continuously varying load. Therefore, this paper applies the CVT as transmission device to the previously proposed system to achieve continuous adjustment of the speed ratio. In addition, an instantaneous optimization control strategy based on the minimum equivalent energy consumption is proposed to reduce the gas consumption and the torque distribution of the engine and the motor and the variation of the CVT ratio under different operating modes are investigated.

2. HPGHP SYSTEM DESCRIPTION

The HPGHP system is mainly comprised of two subsystems: drive system and heat pump system, as shown in Figure 1. The drive system consists of a gas engine and a motor, both of them have a clutch connect to power coupler and then drive the compressor by means of CVT. The dual-use motor as an auxiliary power obtains electric energy from the battery pack to adjust the real-time speed and torque of the engine, so as to ensure the engine running in the economic area. The effect of the power coupler is to transmit the power from the engine and the motor to the CVT at the same speed. Heat pump system is similar to the conventional electric drive refrigeration cycle which mainly includes compressors, outdoor heat exchangers, indoor heat exchangers and expansion valves.

^{*}School of Energy and Environment, Southeast University, 2 Sipailou Street, Xuanwu District, Nanjing, 210096, China.

¹Corresponding author;
Tel. No.: +86 13625170114
E-mail: chentaopipi@126.com.

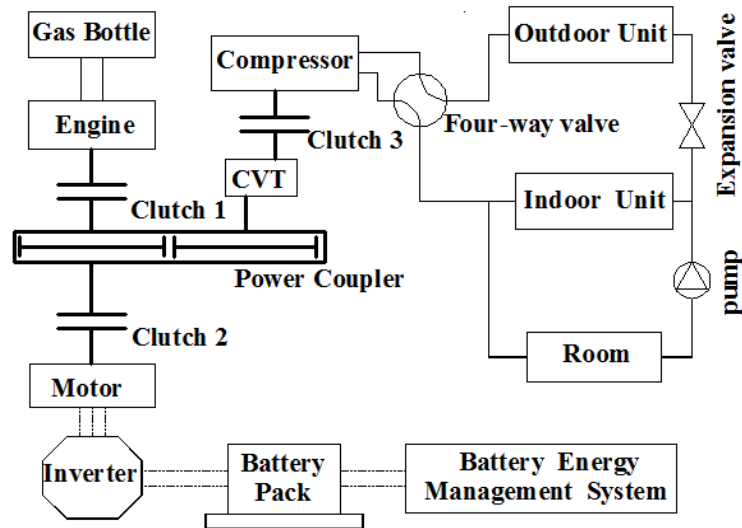


Fig. 1. Schematic diagram of the parallel hybrid-power gas engine heat pump system.

Table 1. Specification of main devices.

Device name	Model parameters	Value
Gas engine	Type	LJ276M Four-stroke
	Speed range	500-4800rpm
	Maximum torque/speed	31.9Nm(2900-3100rpm)
Battery	Type	Lead-acid 6FM-100A
	Number of modules	10
	Rated voltage/ current	12V/100A
Motor	Type	PMSM
	Rated voltage/ current	60V/50A
	Rated speed	3000rpm
	Maximum torque	72Nm
Compressor	Type	BITZER 4UFRY
	Speed range	500-2600rpm
	Rated speed	1480rpm
	Refrigerant	R134a
	Refrigerant lubricants	Bitzer BSE55 POE

Through the clutch open and close, the heat pump system can be driven by the engine and motor separately or together. Through rational allocation of energy management control strategies, the HPGHP system has the following three main operating modes:

Mode D: engine works alone in the economic zone when the output can meet the load demand.

Mode C: engine runs in the economic zone and charges the excess energy to battery pack by the motor that can be used as a generator.

Mode L: engine drives the compressor together with the motor that obtains electrical energy from the battery.

3. MODELING OF DRIVING SYSTEM

According to the engine performance test data, the thermal efficiency of the gas engine is regarded as the binary function of the gas engine speed and the torque by the experimental modeling method. With the aid of the multiple linear regression theory [13], thermal

efficiency characteristic curve of the engine can be established as Equation 1.

$$\begin{cases} \eta_e = [1 \ \omega_e \ T_e \ \omega_e^2 \ \omega_e T_e \ T_e^2] \cdot A_b \\ A_b = [-1.4115 \ 1.8403E-4 \ 0.0931 \ -2.968E-8 \ -2.2888E-7 \ -0.0015] \end{cases} \quad (1)$$

The external characteristic curve and optimum torque curve of the engine can be fitted as follows:

$$T_e = -2.1961 \times 10^{-6} \omega_e^2 + 0.0136 \omega_e + 10.6565 \quad (2)$$

$$T_{opt} = 1.964 \times 10^{-3} \omega_e + 23.6 \quad (3)$$

The universal characteristics curve can be obtained by the contour method, as shown in Figure 2. The circular curve is isothermal efficiency curve; innermost layer is high efficiency, the more outward, the lower the efficiency. As can be seen from the diagram, the maximum thermal efficiency is about 0.279, and the corresponding torque and speed are 29.4 Nm, 3060 rpm, respectively.

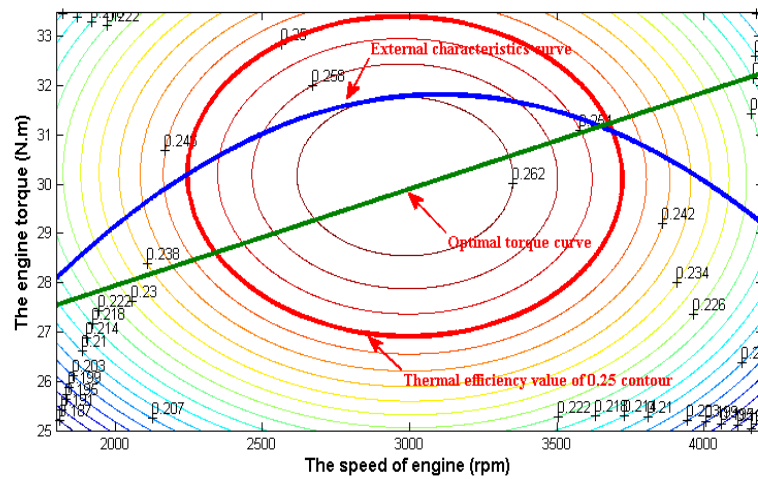


Fig. 2. The universal characteristic curve of engine.

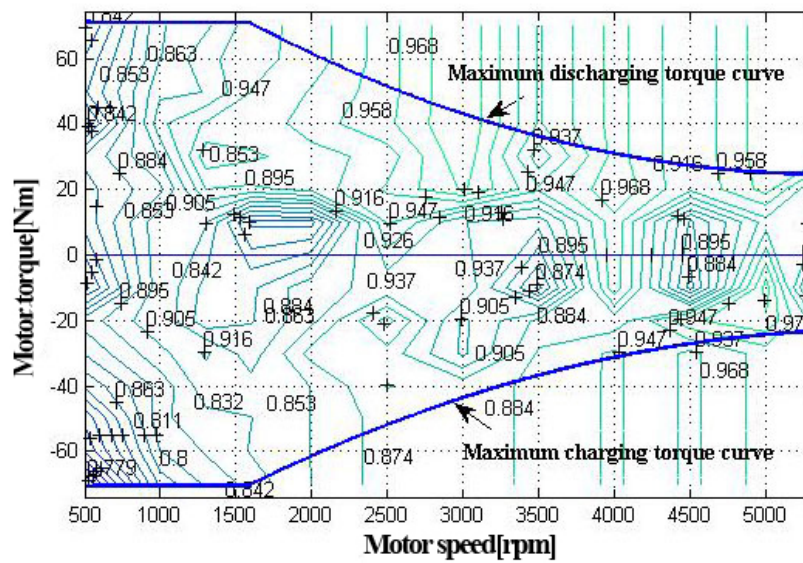


Fig. 3. The motor efficiency map.

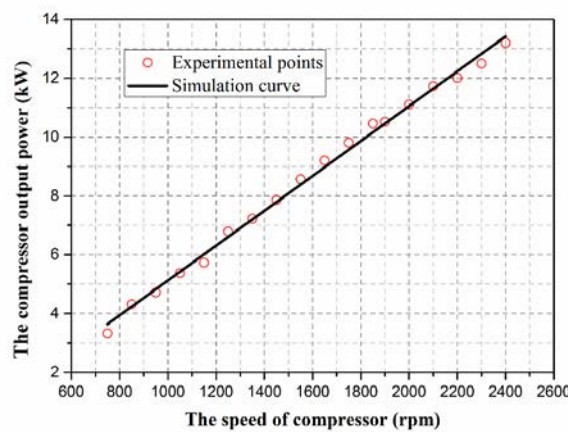


Fig. 4. The relation of compressor output power and compressor speed.

Using the similar method, the motor charge and discharge efficiency map can be obtained, as shown in Figure 3. No matter in charging or discharging state, the motor can maintain high efficiency in the range of 2400 rpm to 3800 rpm, almost keep above 0.9.

The energy transfer between the heat pump system and the drive system can be described by the output

characteristics of the compressor, as shown in Figure 4. The output power of compressor increases approximately linearly with the speed of compressor, the relationship between the two can be expressed as Equation 4:

$$P_c = 0.00575n_c - 0.52934 \quad (4)$$

4. EQUIVALENT ENERGY CONSUMPTION MINIMIZATION CONTROL STRATEGY

Equivalent energy consumption minimization control strategy (EECM-CS) with minimum equivalent energy consumption as the optimization objective is to control the continuous speed ratio of CVT and obtain the optimal torque of the engine and motor to achieve the optimization of the current working point. The minimum equivalent energy consumption is to optimize the energy distribution of the engine and the motor under instantaneous operating conditions, minimizing the total energy consumption of the entire system. The total energy includes the energy consumption of the gas and the energy consumption of the battery.

4.1 Establishment and Description of EECM-CS

4.1.1. Establishment and Description of EECM-CS

The engine and the motor are coaxial connected, so they have the same speed. At any time, the relationship between the drive system and the compressor can be expressed as in Equation 5.

$$\begin{cases} \omega_e(t) = \omega_m(t) = i_{cvt}(t) \cdot \omega_c(t) \\ (T_e(t) + T_m(t)) \cdot i_{cvt}(t) \cdot \eta_{cvt} = T_c(t) \end{cases} \quad (5)$$

where i_{cvt} is the transmission ratio of CVT; η_{cvt} is the transmission efficiency of CVT, whose value is 0.9. Define u as the ratio of the compressor power from the engine to the total demand power of the compressor, $u(t) = T_e(t) \cdot i_{cvt} \cdot \eta_{cvt} / T_c(t)$. The torque of the engine and the motor can be regarded as the function of $u(t)$ and $i_{cvt}(t)$:

$$T_e(t) = \frac{u(t) \cdot T_c(t)}{i_{cvt}(t) \cdot \eta_{cvt}} \quad (6)$$

$$T_m(t) = (1 - u(t)) \frac{T_c(t)}{i_{cvt}(t) \cdot \eta_{cvt}} \quad (7)$$

So, when $u(t)=1$, the power to drive the compressor is all from the engine, the system is in the engine drive compressor alone (mode D); when $u(t)>1$, the output power of the engine is greater than the demand power of the compressor, the engine drives the compressor and charges the battery (mode C); when $u(t)<1$, the output power of the engine is not sufficient to drive the compressor, the system is in the mode of engine and motor driving the compressor together (mode L).

4.1.2. Establishment and correction of objective function

The main purpose of EECM-CS is to optimize the value of u in each instantaneous condition so that the energy consumed of the driving system can be minimized. When the battery is discharged at a certain time, the energy used to drive the compressor comes from the engine and the battery, the engine consumes some of the gas and the battery consumes part of the electricity power. In order to maintain the SOC of battery within the specified range, the power consumption of battery must be replenished by the energy consumption of the gas engine at a future time. That is to say, this part of the electric energy is equivalent to some of gas energy [28]. Similarly, battery charging means that can save some of the gas energy in the future.

So, the objective function of the EECM-CS can be expressed as:

$$Q_{total} = \min(Q_e(t) + K \cdot Q_{b-eq}) \quad (8)$$

where, Q_e is the instantaneous gas energy consumption of engine, Q_{b-eq} is the equivalent gas energy consumption of battery, K is penalty function factor.

The instantaneous engine energy consumption was computed from:

$$Q_e(t) = H_l \cdot G_e = \frac{P_e(t)}{\eta_e(t)} = \frac{T_e[u(t), i_{cvt}(t)] \cdot \omega_e(t)}{9550 \cdot \eta_e(t)} \quad (9)$$

In order to establish the relationship between the battery energy consumption and the equivalent gas energy Q_{b-eq} , the equivalent energy conversion flow path in the battery charging and discharging mode is plotted, as shown in Figure 5.

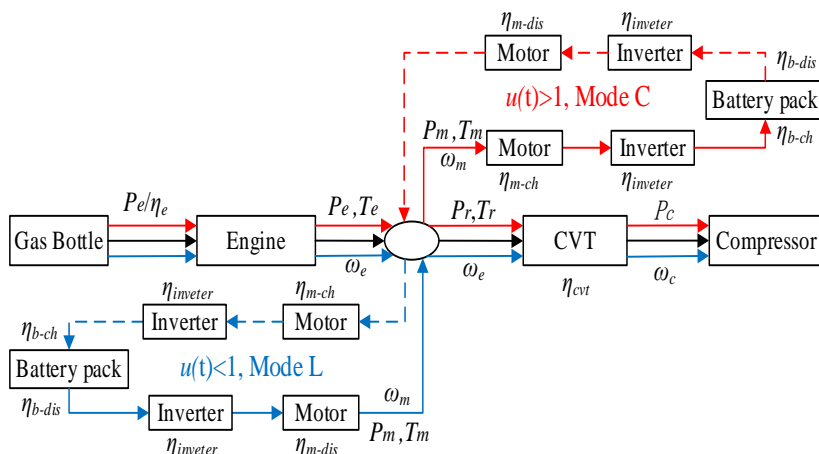


Fig. 5. Energy conversion flow path when charging and discharging.

The red line portion shows the energy flows when the gas engine drives the compressor and charges the battery (solid line part) and the energy flows of the battery packs discharge in the future to keep the SOC stable (dotted line part).

The black line portion represents the energy flow that the gas engine drives the compressor alone, and the battery packs does not participate in its operation.

The blue line portion shows the energy flows of the engine and the motor drive the compressor together

(solid line part), the electric consumption of the battery packs will be compensated by charging driven by gas engine in the future (dotted line part).

According to the description in Figure 5, the calculation formula of Q_{b-eq} can be expressed as following:

When charging ($u(t) > 1$), Q_{b-eq} can be calculated by Equation 10. When discharging ($u(t) \leq 1$), Q_{b-eq} can be obtained by Equation 11.

$$Q_{b-eq} = \frac{P_b \cdot \eta_{b-dis} \cdot \eta_{inverter} \cdot \eta_{m-dis}}{\eta_e} = \frac{T_m \cdot \omega_m \cdot \eta_{m-ch} \cdot \eta_{b-ch} \cdot \eta_{b-dis} \cdot \eta_{inverter}^2 \cdot \eta_{m-dis}}{9550\eta_e} \tag{10}$$

$$Q_{b-eq} = \frac{P_b}{\eta_{b-ch} \cdot \eta_{inverter} \cdot \eta_{m-ch} \cdot \eta_e} = \frac{T_m \cdot \omega_m}{9550\eta_{m-dis} \cdot \eta_{b-dis} \cdot \eta_{b-ch} \cdot \eta_{inverter}^2 \cdot \eta_{m-ch} \cdot \eta_e} \tag{11}$$

Table 2. Values of the different parameter symbol.

Battery discharge efficiency	Battery charge efficiency	Inverter efficiency
η_{b-dis}	η_{b-ch}	$\eta_{inverter}$
0.94	0.87	0.9

where η_{m-ch} and η_{m-dis} are the charge and discharge efficiencies of the motor, respectively, which can be achieve from the Figure 3. The values of the other parameter symbol appeared in Equations 10 and 11 are given in Table 2.

The penalty function is proposed to revise the equivalent energy consumption and adjust the tendency of electric energy usage to maintain the battery SOC within a reasonable range, as shown in Figure 6. The shape of the curve can be adjusted by modifying the coefficients a, b and c, whose value are 16.35, 30.15, 152.3, respectively. The correction formula of penalty function can be expressed as:

$$D_{SOC} = SOC - \frac{SOC_{min} + SOC_{max}}{2} \tag{12}$$

$$K = \begin{cases} 1 - a \cdot D_{SOC}^4 & D_{SOC} \geq 0 \\ 1 - b \cdot D_{SOC}^3 + c \cdot D_{SOC}^4 & D_{SOC} < 0 \end{cases} \tag{13}$$

where, SOC_{min} and SOC_{max} are the lower and upper limits of the SOC value of the battery, respectively.

Through the above analysis, the constraints of the objective function can be defined as in Equation 14.

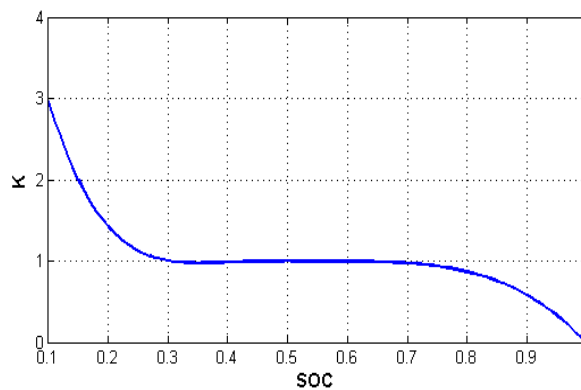


Fig. 6. Penalty function of SOC.

$$\begin{cases} Q_{total} = \min(Q_e[u(t), i_{cvt}(t)] + K \cdot Q_{b-eq}[u(t), i_{cvt}(t)]) \\ \max\left(\frac{T_{e_min} \cdot i_{cvt} \cdot \eta_T}{T_c}, 1 - \frac{T_{m_max} \cdot i_{cvt} \cdot \eta_T}{T_c}\right) \leq u(t) \leq \min\left(\frac{T_{e_max} \cdot i_{cvt} \cdot \eta_T}{T_c}, 1 - \frac{T_{m_min} \cdot i_{cvt} \cdot \eta_T}{T_c}\right) \\ i_{cvt_min} \leq i_{cvt}(t) \leq i_{cvt_max} \\ \omega_{e_min} \leq \omega_e \leq \omega_{e_max} \\ T_{e_min} \leq T_e \leq T_{e_max} \\ SOC_{min} \leq SOC(t) \leq SOC_{max} \end{cases} \tag{14}$$

4.2 Optimization and Analysis of Control Strategy

4.2.1. Establishment and Description of EECM-CS

The execution flow chart of the equivalent energy consumption minimization control strategy is shown in Figure 7. The compressor demand speed ω_c and the value of current SOC as the identification parameters of the entire system, according to the compressor model to obtain its torque value T_c and penalty function. The engine speed ω_e at a certain transmission ratio can be calculated from the model of CVT. If the engine speed is outside the economic zone, then jump to the next

transmission ratio until the engine speed meet the requirements. The maximum and minimum torque of engine and motor at certain ω_e (The motor is coaxially connected with engine and has the same speed) can be obtained by the model of engine and motor, and then the range of variable u is calculated. Comparing the relationship between u and 1 selects the corresponding drive mode and calculates the total energy consumption. Repeat the cycle to calculate the energy consumption of all u values under a certain i_{cvt} and obtain the minimum value of energy consumption, thus the minimum energy value of all i_{cvt} and u are obtained.

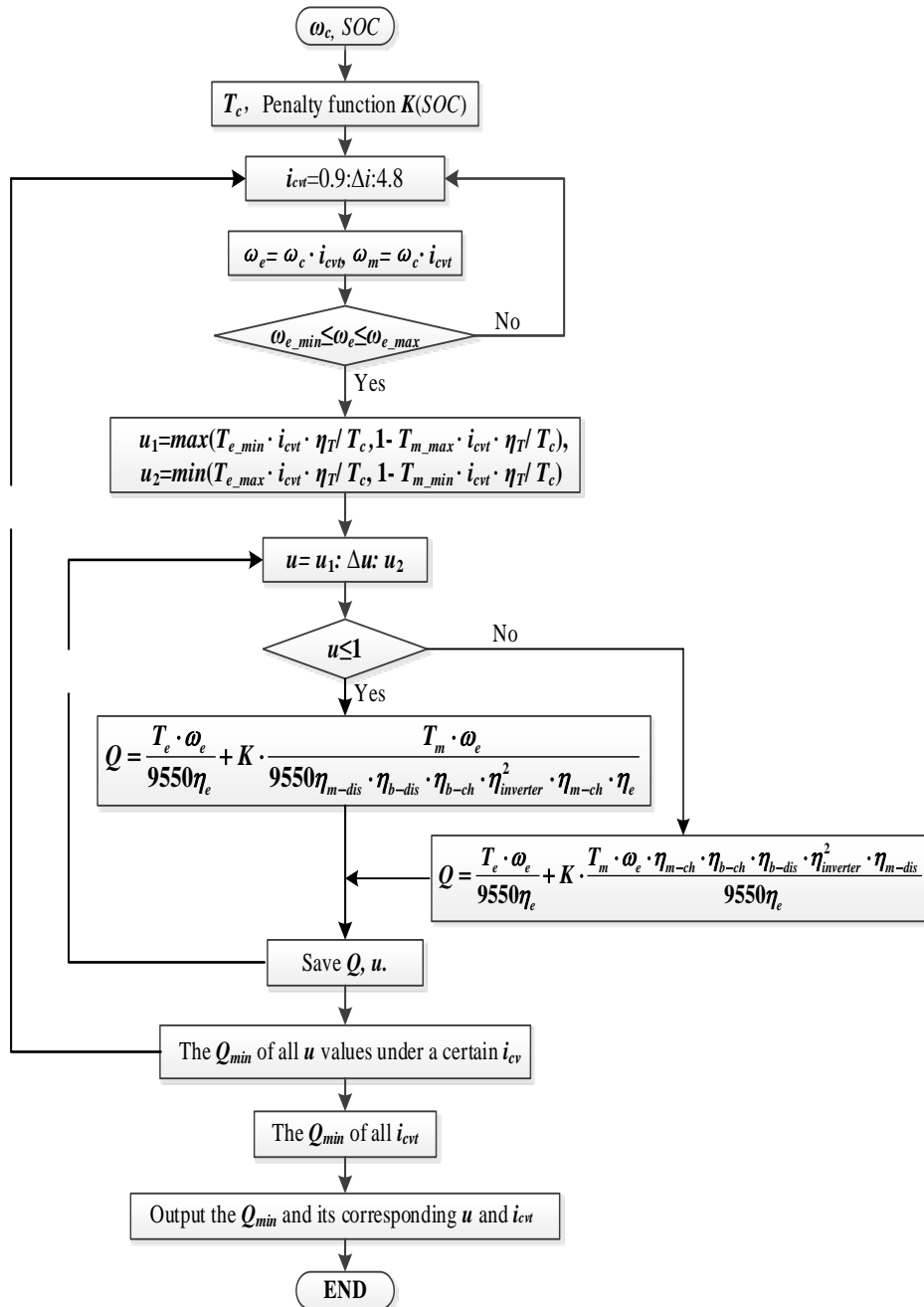


Fig. 7. The flow chart of the EECM-CS.

For different compressor speeds, the optimization results of u and i_{cvt} are shown in the Figure 8. From the value of u , we can see that when the compressor speed is 1350rpm, the drive system converted from mode C to

mode D, and when the compressor speed is 1800 rpm, the drive is switched from mode D to mode L. The values of CVT in three modes are 3.4-2.1, 2.1-1.9, and 1.9-1.2, respectively.

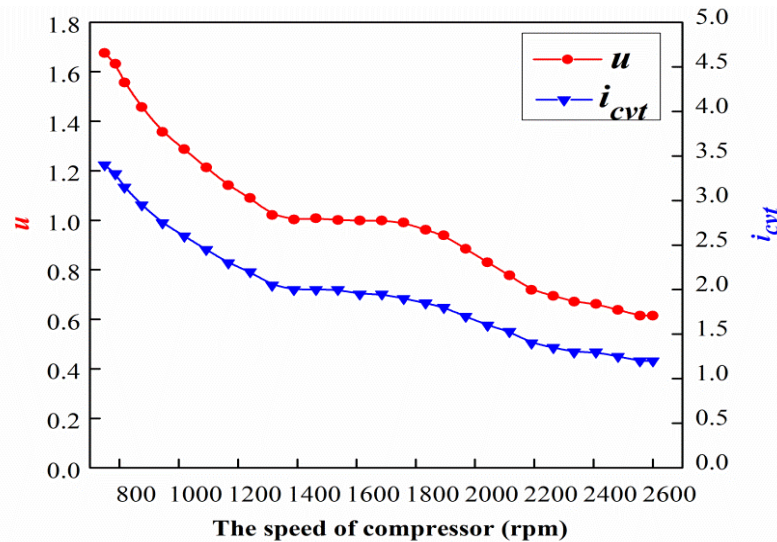


Fig. 8. The curve of u and i_{cvt} with compressor speed.

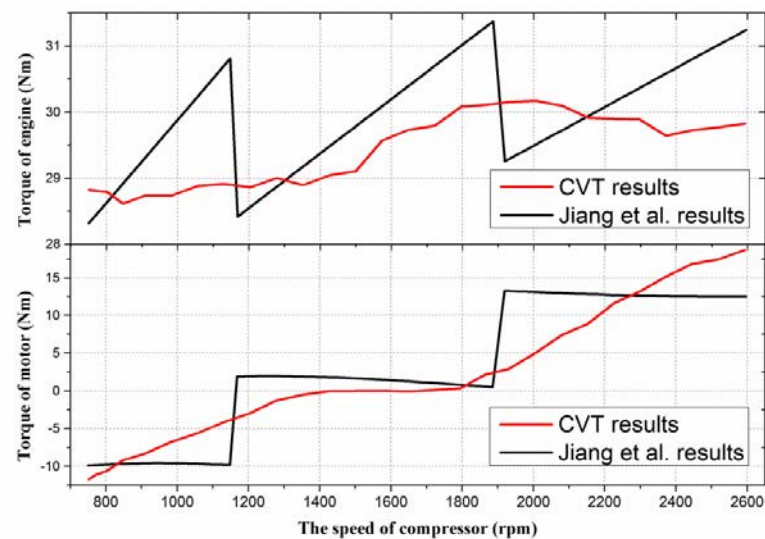


Fig. 9. Torque distribution under EECM-CS.

4.2.2. Optimization result

The torque distribution of engine and motor in different modes is shown in the Figure 9. In mode C, with the compressor rotation speed increases, the output torque of the engine is maintained at about 28.7 N·m by adjusting the gear ratio of the CVT, and the charging torque of motor becomes smaller and smaller, from -11 N·m to -1.2 N·m (negative means charging). In mode D, the energy provided by the engine itself can meet the change in the demand load, with the stepless speed regulation of the CVT, the engine operates on the optimal torque curve of the economic zone, with a slight increase in torque from 29 N·m to 30.2 N·m. In mode L, as the demand load increase, the motor continuously increases its torque output (from 2.1 N·m to 18.7 N·m) to keep the engine running economically (maintained at 29.8 N·m).

In order to evaluate the energy distribution effect of the system after using CVT, the torque value of the engine and the motor is compared with the result of Jiang's multi-stage transmission ratio system [11].

Compared to the sawtooth torque, the torque of the engine can be controlled in a small range of 28.7 N·m to 30.17 N·m by means of the high charge and discharge efficiency of motor in larger torque range and the continuous speed regulation of the CVT. The average operating efficiency of the engine in this range is significantly higher than that of the multi-stage transmission.

The curve of SOC value based on EECM-CS is shown in Figure 10. It can be seen that when the system is operating in mode C, the engine converts the excess gas heat energy into electrical energy stored in the battery. Due to the application of the penalty function to limit the charge of the battery to the engine, the growth rate of SOC is slower, from the initial value of 0.6 to 0.63. When running in mode D, the motor does not work, the value of battery SOC unchanged; In mode L, the battery is discharged to compensate for the insufficient of engine energy supply, the penalty function promotes the battery to discharge, and its SOC value drops rapidly from 0.63 to 0.5.

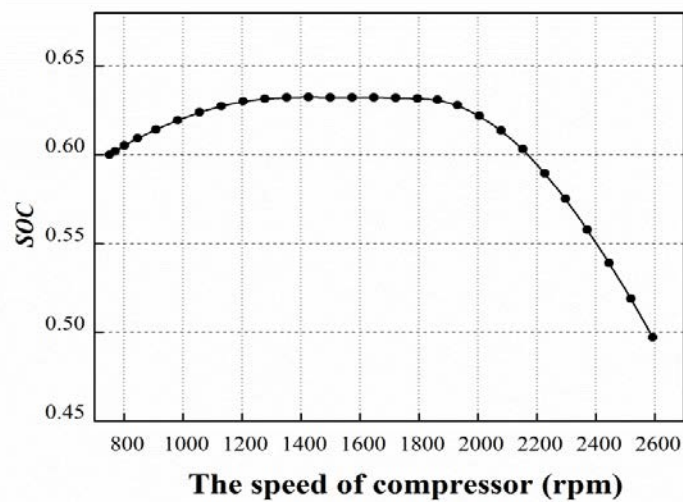


Fig. 10. SOC change curve under EECM-CS.

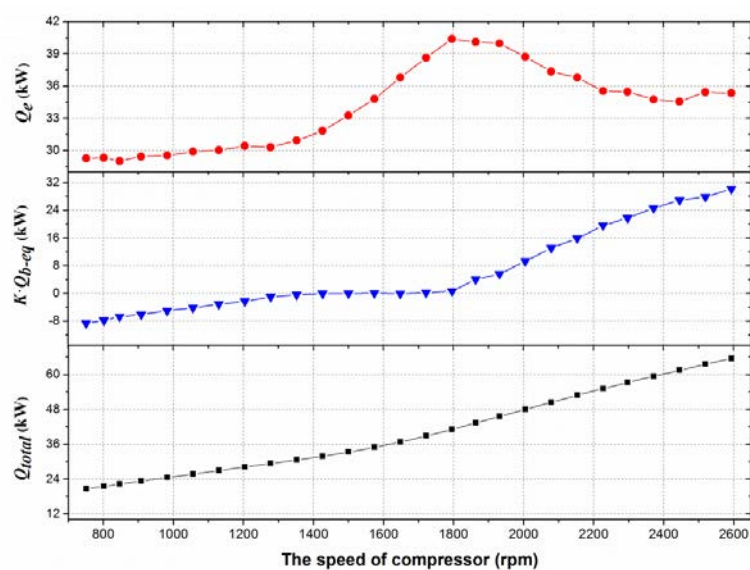


Fig. 11. Energy distribution at different compressor speeds.

Figure 11 shows the energy distribution at different compressor speeds. The ordinate from top to bottom is the engine energy consumption, the equivalent energy consumption of battery and the total energy consumption, respectively. With the demand load increasing, the total energy consumption increased from 20.6 kW increase to 65.5 kW. Through the continuous speed control of the CVT, the speed and torque of the engine fluctuates in a small range, which can reduce its energy consumption. As shown in the figure, when running in mode C and mode L, the motor bears the excess and insufficient energy of the engine, so that the output power of engine can be maintained at a relatively stable value of 29.5kW and 34.5 kW, respectively. In mode D, the energy provided by engine is all used to drive the compressor, gradually increasing from 29.5 kW to 40.4 kW, and then decreasing to 34.5 kW as mode D switches to mode L. Due to the application of the penalty function, the equivalent energy of the battery changes slowly from -8.5 to 0.37 kW in mode C, and increases rapidly from 4.1 kW to 30.2 kW in the mode L.

4.3 Comparison and Analysis

For more comprehensive assessment of the economics of HPGHP system under EECM-CS and CVT applications, the result of gas consumption rate compared with Wang's [7] research data are shown in Figure 12. With the increase of the compressor speed in different working modes, the gas consumption rate under CVT fluctuates within a small range, which is obviously lower than that of Wang's multi-stage driving system. The minimum gas consumed rate of mode C, mode D and mode L is 283.6 g/(kWh), 283.6 g/(kWh), and 281.3 g/(kWh), respectively. In addition, the average gas consumed rate of Wang's result in the three modes is 291.4 g/(kWh), 293.1 g/(kWh) and 294.3 g/(kWh), and the average gas consumed rate using CVT is 285.5 g/(kWh), 286.3 g/(kWh) and 283.1 g/(kWh), which is lower than that of Wang *et al.* by about 2%, 2.4% and 4%, respectively, indicating that the HPGHP system has good energy saving effect with the application of CVT speed regulation.

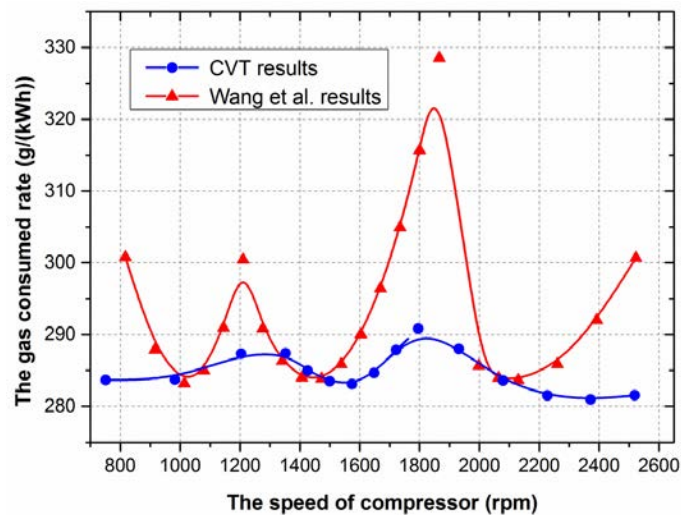


Fig. 12. The relation between the gas consumed rate and compressor speed.

5. CONCLUSIONS

- i. Instantaneous optimal control strategy based on EECM is proposed by converting the energy of the stored/consumed battery equivalent to the engine gas energy. In order to maintain the stability of the battery SOC value, the penalty function is used to modify the energy objective function.
- ii. By judging the value of u , a new switching method of the operating mode of the drive system is established. The results show that the compressor speed of 1350 rpm and 1800 rpm is the switching point of C, D and L mode, and the ranges of i_{cvt} in the three modes are 3.4 to 2.1, 2.1 to 1.9, and 1.9 to 1.2, respectively.
- iii. The engine and the motor torque distribution and gas consumed rate of the engine under EECM-CS are compared and analyzed. By introducing the penalty function to amend the charging and discharging torque of a dual-use motor with high efficiency, the torque of the engine can be controlled in a smaller economic range (28.7 to 30.2 N·m).
- iv. The average gas consumed rate of the engine is 285.5 g/(kWh), 286.3 g/(kWh) and 283.1 g/(kWh) in mode C, mode D and mode L, less than multi-stage transmission system about 2%, 2.4% and 4%, indicating that the HPGHP has good energy saving prospects under the application of CVT and the control of EECM-CS.

ACKNOWLEDGEMENT

The authors gratefully acknowledge the support of China National Key R and D Program (No. 2016YFC0700305) and Postgraduate Research and Practice Innovation Program of Jiangsu Province (No. KYCX17_0114).

REFERENCES

- [1] Hepbasli A., Erbay Z. and Icier F., 2009. A review of gas engine driven heat pumps (GEHPs) for residential and industrial applications. *Renewable and Sustainable Energy Reviews* 13(1): 85 – 99.
- [2] Sanaye S., Chahartaghi M., and Asgari H., 2013. Dynamic modeling of gas engine driven heat pump system in cooling mode. *Energy* 55(1): 195 – 208.
- [3] Elgendy E., Schmidt J., and Khalil A., 2011. Performance of a gas engine driven heat pump for hot water supply systems. *Energy* 36(5): 2883 – 2889.
- [4] Gungor A., Tsatsaronis G., and Gunerhan H., 2015. Advanced exergoeconomic analysis of a gas engine heat pump (GEHP) for food drying processes. *Energy Conversion and Management* 91: 132 – 139.
- [5] Li Y.L., Zhang X.S. and Cai L., 2007. A novel parallel-type hybrid-power gas engine-driven heat pump system. *International Journal of Refrigeration* 30(7): 1134 – 1142.
- [6] Li Y.L., Cai L. and Zhang X.S., 2006. Hybrid power gas engine-driven heat pump system and technical analysis. *Journal of HV and AC* 36(11): 11 – 13.
- [7] Wang Y., Cai L. and Yu Y., 2013. Performance study of parallel-type hybrid-power gas engine-driven heat pump system. *Energy and Buildings* 62: 37-44.
- [8] Won J.S., Langari R. and Ehsani M., 2005. An energy management and charge sustaining strategy for a parallel hybrid vehicle with CVT. *IEEE Transactions on Control Systems Technology* 13(2): 313 – 320.
- [9] Ji J., Park K., and Kwon O., 2012. An energy management strategy for a CVT based parallel hybrid electric vehicle. In *Proceedings of 2012 IEEE Vehicle Power and Propulsion Conference*. IEEE, pp, 380-382.
- [10] Wang J., Cai L. and Wang Y., 2013. Modeling and optimization matching on drive system of a coaxial parallel-type hybrid-power gas engine heat pump. *Energy* 55: 1196 – 1204.
- [11] Wang J., Cai L. and Wang Y., 2015. Simulation and validation of a hybrid-power gas engine heat pump. *International Journal of Refrigeration* 50: 114 – 126.

- [12] Chen T., Cai L. and Wan X., 2017. Modeling and dynamic energy management control of hybrid-power gas engine heat pump system. *Applied Thermal Engineering* 121: 585 – 594.
- [13] Zhou G., Hao Z. and Liu R., 2009. Universal characteristics curve plotting method based on MATLAB. *Internal Combustion Engine and Powerplant* 2: 007.